JACS
JOURNAL OF THE AMERICAN CHEMICAL SOCIETY
Communication
pubs.acs.org/JACS

Chasing Changing Nanoparticles with Time-Resolved Pair Distribution Function Methods

Mark A. Newton,*[,†] Karena W. Chapman,*[,‡] David Thompsett,[§] and Peter J. Chupas*[,‡]

[†]European Synchrotron Radiation Facility, 6, Rue Jules Horowitz, BP-220, Grenoble, F-38043, France
[‡]X-ray Science Division, Advanced Photon Source, Argonne National Laboratory, Argonne, Illinois 60439, United States
[§]Johnson Matthey Technology Centre, Sonning Common, Reading, RG4 9NH, United Kingdom

Supporting Information

ABSTRACT: When materials are reduced to the nanoscale, their structure and reactivity can deviate greatly from the bulk or extended surface case. Using the archetypal example of supported Pt nanoparticles (ca. 2 nm diameter, 1 wt % Pt on Al_2O_3) catalyzing CO oxidation to CO_2 during cyclic redox operation, we show that high energy X-ray total scattering, used with subsecond time resolution, can yield detailed, valuable insights into the dynamic behavior of nanoscale systems. This approach reveals how these nanoparticles respond to their environment and the nature of active sites being formed and consumed within the catalytic process. Specific insight is gained into the structure of the highly active Pt surface oxide that formed on the nanoparticles during catalysis.

When constrained to ever smaller dimensions, many materials yield chemical and physical properties that are very different from their bulk analogues. Often these distinct properties are of considerable value in a wide range of technological applications.[1−4] Indeed, a majority of heterogeneous catalysts that are used commercially to refine raw fuel stocks, act as sensors, combat environmental pollution, or produce energy rely on highly dispersed nanoparticles (<5 nm diameter) of metals and/or metal oxides. Such nanoparticles are not passive; they adapt dynamically to their environment as they facilitate catalytic conversions. Thus, the quantitative elucidation of their structure and reactive properties presents a significant challenge, requiring in situ probes that can be applied on suitable time scales.[5] While the catalytic oxidation of CO to CO_2 has been studied for almost a century, for both fundamental and applied reasons,[6,7] the detailed picture of how this "simple" conversion is achieved continues to be an active area of research.[8−16] This exemplifies the challenge in definitively resolving the relation between structure and function.

Here we show how pair distribution function (PDF) methods can interrogate a dilute and dynamic catalytic system in situ, by studying 1 wt % Pt on Al_2O_3 catalyzing CO oxidation during cyclic "redox" operation. This approach allows the structure of the nanoparticles to be probed as they are working. Insight is gained into the dynamic structure and reactivity of active Pt phases that cannot otherwise be obtained.

PDF analysis provides local structural information with atomic resolution from the immediate coordination environment (a few Å) up to several nanometers; spanning the entire length scale of nanoparticles relevant to catalysis.[17−24] An advantage of PDF over EXAFS (extended X-ray absorption fine structure) analysis is that insights are not limited to the immediate coordination environment.[20] Thus, the PDF method yields a structural description of materials that bridges a very important blind spot—between 5 and 20 Å—that exists between EXAFS and Bragg diffraction/small angle scattering. Third generation synchrotron sources, together with advances in detector technology,[25] have enabled time-resolved PDF studies to probe systems such as supported metal catalysts in situ.[26]

High energy X-ray scattering data suitable for PDF analysis were collected for a 1 wt % Pt in Al_2O_3 catalyst within a capillary-based microreactor[27] at 500 K. The sample was subjected to a gas flow that switched between stoichiometric (*stoich*; $2CO{:}O_2$) and oxidizing (*ox*; $CO{:}5O_2$) feedstocks every 30 s. Data were collected at 1 s intervals. Data were also collected at shorter intervals (0.25 s) to check for changes that may occur at this faster time scale. Differential PDFs (d-PDFs) were obtained by subtracting the contribution of the Al_2O_3, isolating the PDF corresponding to the Pt nanoparticles (Figure 1). The differential data can be modeled as nanoparticles of ∼2 nm diameter with a face-centered cubic structure in good agreement with TEM (see Supporting Information).[28] While there are limitations in the fcc model,

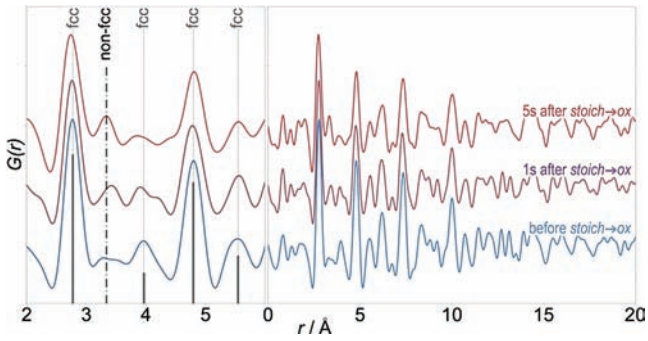

Figure 1. Differential PDFs for the Al_2O_3-supported Pt catalyst upon switching from *stoich* to *ox* feedstocks. The expanded *r*-region roughly matches the range typically probed using EXAFS.

Received: December 6, 2011
Published: March 7, 2012

particularly beyond ~10 Å, a limited *r*-range fit suggests a modest reduction in the coherent particle size (by ~2.5 Å), under *ox* conditions.

The d-PDFs obtained under *stoich* and *ox* conditions indicate several distinct changes upon switching feedstock (Figure 1). Under *ox* conditions, peaks in the PDF systematically broaden, the average nearest neighbor peak (~2.75 Å) shifts to shorter distance, and a non-fcc feature appears at ~3.3 Å .

Gaussian functions were fit to individual features in the d-PDFs to quantify these structural changes and to identify correlations (Figure 2). This analysis indicates that the

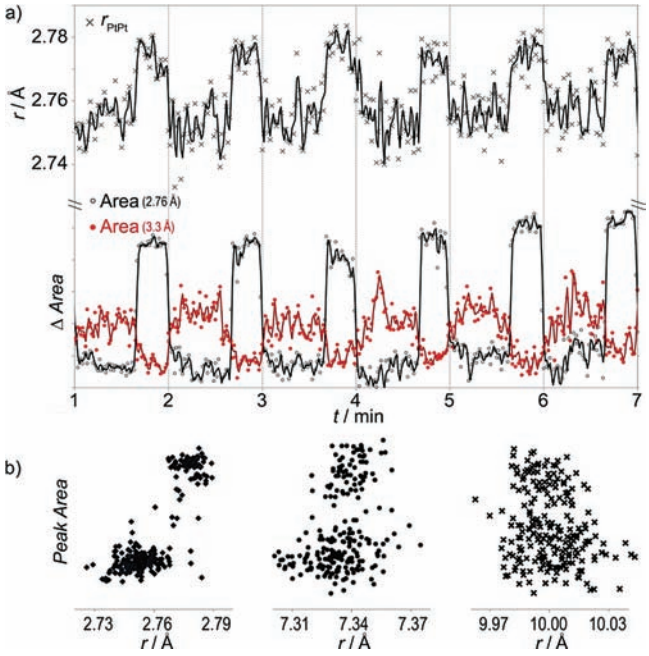

Figure 2. (a) The average Pt−Pt bond length (at ~2.75 Å) and corresponding peak area during switching between *stoich* and *ox* feedstocks. The area of the non-fcc peak (at 3.3 Å) shows an inverse trend. (b) While the direct Pt−Pt bond length and peak area are correlated, fcc features at high *r* modulate in intensity without systematic changes in distance.

nanoparticles adapt rapidly and reversibly to the modulated chemical environment. While all distinct fcc features broaden or attenuate in response to their modulated environment, it is only for the first Pt−Pt distance that this change is accompanied by a systematic concomitant change in distance. Interestingly, while the sample was exposed to *stoich* and *ox* flows for equal durations, the time-dependence of the structural parameters indicates that under *stoich* conditions it takes longer (35 s) for the structure to reach a steady state.

The principal indicator of catalytic activity, CO_2 production, was correlated with structural parameters from the PDF analysis (Figure 3). The steady-state CO_2 production is strongly linked to the intensity of the non-fcc feature at ca. 3.3 Å; under *stoich* conditions, where the 3.3 Å feature is smallest, CO_2 production is ca. two-thirds that under *ox* conditions. The greater CO_2 productivity under *ox* conditions occurs despite a lower CO concentration in the feed. Accordingly, the nanoparticle structure that exists under *ox* conditions appears to be more efficient at CO elimination. A brief surge in CO_2 production accompanies the transition between the two Pt nanoparticle states upon gas switching,

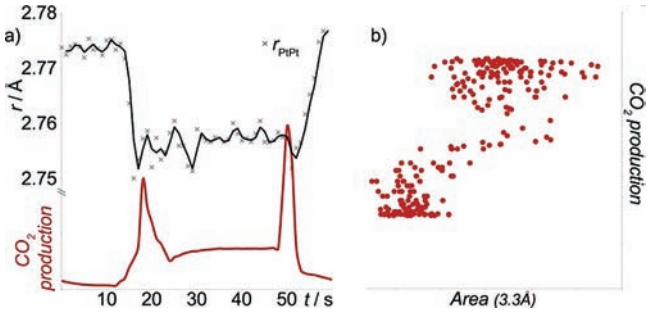

Figure 3. (a) The CO_2 production and average Pt−Pt bond length through a single redox modulation. (b) The steady-state CO_2 production is correlated with the non-fcc feature at 3.3 Å.

after which the CO_2 production rapidly stabilizes. These observations are consistent with previous studies; they reflect the competitive binding of CO and O_2 at the surface and the dynamic equilibrium between free and adsorbed gas molecules.[5−16] Under the CO rich *stoich* feed, surface sorption is dominated by CO, blocking O_2 sorption, hence, inhibiting O_2 dissociation and CO oxidation. Upon switching to the O_2 rich/CO poor *ox* feed, the equilibrium shifts to favor CO desorption, liberating surface sites for the dissociation of O_2, producing a surge in CO_2 formation. Subsequently, a new equilibrium is rapidly established wherein O_2 competes more effectively with CO for surface sites and enhanced CO turnover occurs. The longer delay in attaining a steady state under *stoich* conditions suggests that the removal of oxygen from the surface oxide layer needs to occur prior to binding of the CO.

The consistency of the fcc features in the d-PDF indicates that the core nanoparticle structure is largely retained through the reaction. Upon switching to the *ox* feed, changes in the d-PDF are localized at low *r*, suggesting that only short-range structural changes occur—likely oxidation at the particle surface. The general broadening of the fcc features under *ox* conditions likely reflects additional strain within the nanoparticle, possibly induced by the surface oxide formation.

To more clearly visualize the restructuring of the Pt nanoparticle surface associated with increased catalytic activity, a further differential PDF was computed, subtracting the d-PDF obtained under *stoich* conditions from that obtained under *ox* conditions—a "surface" differential PDF.[29] This differential approach can successfully recover even highly dilute surface features as artifacts in the PDFs largely cancel in the differential. Several distinct structural features are evident in the surface differential at 3.3 Å and also at 2.0, 2.6, and 4.4 Å. In the d-PDF of the nanoparticle, the feature in the surface differential at 2.6 Å is not resolved from the Pt−Pt bond length in the fcc structure. The varying contribution from the shorter surface correlation underlies the observed changes in the feature at ~2.75 Å. A feature at 2.6 Å has been observed, but not identified, in EXAFS studies from related oxidized Pt catalysts.[13,30]

Although the PDF provides no direct information on the identity of the atoms associated with each peak, based on the relative intensity of different types of correlations and known bond lengths, a credible model of the surface structure can be devised. In this system, correlations involving the strongly scattering Pt atoms dominate the PDF, with strong Pt−Pt and weaker Pt−O correlations. The small peak at 2.0 Å corresponds to a typical Pt−O bond length. This, and several other peaks in the surface differential, can be matched to distances in an AB-

dx.doi.org/10.1021/ja2114163 | *J. Am. Chem. Soc.* 2012, 134, 5036−5039

stacked close-packed arrangement of Pt and O layers (see Figure 4). In this model, the peaks at 2.6 and 4.4 Å correspond

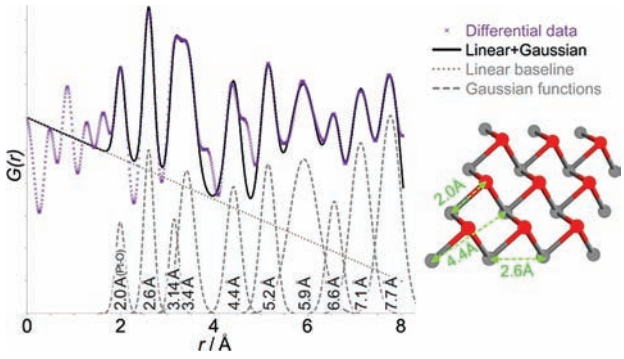

Figure 4. A surface differential PDF $(G(r)_{ox} - G(r)_{stoich})$ corresponding to the structure generated in oxidizing conditions. Gaussian functions fit to correlations in the data suggest that it is consistent with a two-dimensional PtO_2 layer over an fcc lattice.

to the nearest and next-nearest neighbor Pt···Pt distances. The triply bridging O atom is likely associated with the short 2.6 Å Pt−Pt distance Thus, the surface differential can be described by an oxidized Pt surface with close-packed Pt and O layers, not globally coherent with the bulk nanoparticle. The data do not indicate whether the surface oxide exists as a continuous layer or as remote islands. We propose that relaxation of this partially oxidized hexagonal Pt layer relative to the ordered fcc core gives rise to the longer Pt···Pt distance at 3.3 Å.

Intriguingly, this local structure model, derived for small nanoparticles of comparable dimension to many industrial catalysts, is similar to that observed for quasi-infinite extended surfaces, a model system at the opposite extreme of Pt dispersion. In situ, elevated pressure surface X-ray diffraction studies of extended Pt surfaces indicate a slightly distorted hexagonal layer, having net PtO_2 stoichiometry, that is relaxed away from the remainder of the metal surface to a distance of ca. 3.3(1) Å.[11] As observed here, this incommensurate surface oxide was linked to high CO elimination activity. Other studies on the surface oxidation of Pt single crystals[31−33] have also observed structures with similar Pt−Pt distances.

In summary, we have demonstrated that PDF analysis of total X-ray scattering data can be achieved for in situ measurements of dilute and highly dispersed supported nanoparticles on the second time scale and below. This brings a new and valuable window into how a wide variety of materials behave under real operating conditions. This has allowed us to observe, with unique temporal and structural specificity, how small Pt nanoparticles adapt, in their entirety, to the conditions their surface experience; to identify specific surface structures that are highly correlated to their overall catalytic function; and to demonstrate the similarity that can exist between the supported nanoparticle case and its extended-surface analogues[11] in this most fundamental of all catalytic conversions.

■ ASSOCIATED CONTENT

Supporting Information

Details of sample preparation, TEM characterization, and PDF analysis. This material is available free of charge via the Internet at http://pubs.acs.org.

■ AUTHOR INFORMATION

Corresponding Author

mark.newton@esrf.fr; chapmank@aps.anl.gov; chupas@aps.anl.gov

Notes

The authors declare no competing financial interest.

■ ACKNOWLEDGMENTS

Work done at Argonne and use of the Advanced Photon Source (APS) was supported by the U.S. DOE under Contract No. DE-AC02-06CH11357. We thank P. Harris and L. Felisiari at the Centre for Advanced Microscopy (CfAM), University of Reading, U.K. for the TEM measurements. M.A.N. thanks the Royal Society of Chemistry (RSC) for a Journals grant (09 01 639) funding travel to participate in these measurements, the APS for a visiting scientist position and the ESRF for time to pursue this work.

■ REFERENCES

(1) Halperin., W. P. *Rev. Mod. Phys.* **1986**, *58*, 533.
(2) Che, M.; Bennett, C. O. *Adv. Catal.* **1989**, *36*, 55.
(3) Satoh, N.; Nakashima, T.; Kamikura, K.; Yamamoto, K. *Nat. Nanotechnol.* **2008**, *3*, 106.
(4) (a) Sanchez, S. I.; Menard, L. D.; Bram, A.; Kang, J. H.; Small, M. W.; Nuzzo, R. G.; Frenkel, A. I. *J. Am. Chem. Soc.* **2009**, *131*, 7040. (b) Newton, M. A. *Chem. Soc. Rev.* **2008**, *37*, 2644.
(5) Langmuir, I. *J. Am. Chem. Soc.* **1915**, *37*, 116.
(6) Langmuir, I. *Trans. Farad. Soc.* **1922**, *17*, 621.
(7) Yeates, R. C.; Turner, J. E.; Gellman, A. J.; Somorjai, G. A. *Surf. Sci.* **1985**, *149*, 175.
(8) Wintterlin, J.; Volkening, S.; Janssens, T. V. W.; Zambelli, T.; Ertl, G. *Science* **1997**, *278*, 1931.
(9) Hartmann, N.; Imbihl, R.; Vogel, W. *Catal. Lett.* **1994**, *28*, 373.
(10) Heiz, U.; Sanchez, A.; Abbet, S.; Schneider, W.-D. *J. Am. Chem. Soc.* **1999**, *121*, 3214.
(11) Hendriksen, B. L. M.; Frenken, J. M. W. *Phys. Rev. Lett.* **2002**, *89*, 046101.
(12) Ackermann, M. D.; Pedersen, T. M.; Hendriksen, B. L. M.; Robach, O.; Bobaru, S. C.; Popa, I.; Quiros, C.; Kim, H.; Hammer, B.; Ferrer, S.; Frenken, J. W. M. *Phys. Rev. Lett.* **2005**, *95*, 255505.
(13) Singh, J.; Tromp, M.; Safonova, O. V.; Glatzel, P.; van Bokhoven, J A. *Catal. Today* **2009**, *145*, 300.
(14) Alayon, E. M. C.; Singh, J.; Nachtegaal, M.; Harfouche, M.; van Bokhoven, J. A. *J. Catal.* **2009**, *263*, 228.
(15) Singh, J.; Nachtegaal, M.; Alayon, E. M. C.; Stötzel, J.; van Bokhoven, J. A. *ChemCatChem* **2010**, *2*, 653.
(16) Allian, A. D.; Takanabe, K.; Fujdala, K. L.; Hao, X.; Truex, T. J.; Cai, J.; Buda, C.; Neurock, M.; Iglesia, E. *J. Am. Chem. Soc.* **2011**, *133*, 4498.
(17) Franklin, R. E. *Acta Crystallogr.* **1950**, *3*, 107.
(18) Egami, T.; Billinge, S. J.L. *Underneath the Bragg Peaks: Structural Analysis of Complex Materials*; Pergamon Press: Kiddington, Oxford, U.K., 2003.
(19) Conventional Bragg diffraction does not provide enough information for structural determination of nanoscale materials (e.g., heterogeneous catalysts) as crystallographic reflections are intrinsically broad for particles of less than a few nanometers.
(20) See, for example , Gallezot, P. X-ray techniques in catalysis. In *Catalysis, Science and Technology*; Anderson, J. R., Boudart, M., Eds.; Springer: Berlin, 1984; Vol. *5*, Chapter 4.
(21) See, for example Hall, B. D. *J. Appl. Phys.* **2000**, *87*, 1666.
(22) See, for example Ratnasamy, P.; Leonard, A. J. *Catal. Rev.: Sci. Eng.* **1972**, *6*, 293.
(23) Gallezot, P. *Catal. Rev.: Sci. Eng.* **1979**, *20*, 121.
(24) Liang, K. S.; Laderman, S. S.; Sinfelt, J. H. *J. Chem. Phys.* **1987**, *86*, 2352.

(25) (a) Chupas, P. J.; Chapman, K. W.; Lee, P. L. *J. Appl. Crystallogr.* **2007**, *40*, 463. (b) Chupas, P. J.; Qiu, X.; Hanson, J. C.; Lee, P. L.; Grey, C. P.; Billinge, S. J. L. *J. Appl. Crystallogr.* **2003**, *36*, 1342.
(26) Chupas, P. J.; Chapman, K. W.; Jennings, G.; Lee, P. L.; Grey, C. P. *J. Am. Chem. Soc.* **2007**, *129*, 45.
(27) Chupas, P. J.; Chapman, K. W.; Kurtz, C.; Hanson, J. C.; Lee, P. L.; Grey, C. P. *J. Appl. Crystallogr.* **2008**, *41*, 822.
(28) Korsunskiy, V. I.; Neder, R. B.; Hofmann, A.; Dembski, S.; Graf, C.; Ruhl, E. *J. Appl. Crystallogr.* **2007**, *40*, 975.
(29) Chupas, P. J.; Chapman, K. W.; Halder, G. J. *J. Am. Chem. Soc.* **2011**, *133*, 8522.
(30) Borgna, A.; Le Normand, F.; Garetto, T.; Apesteguia, C. R.; Moraweck, B. *Catal. Lett.* **1992**, *13*, 175.
(31) Helveg, S.; Lorensen, H. T. *Surf. Sci.* **1999**, *430*, L533.
(32) Li, W. X.; Österlund, L.; Vestergaard, E. K.; Vang, R. T.; Matthiesen, J.; Pedersen, T. M.; Lægsgaard, E.; Hammer, B.; Besenbacher, F. *Phys. Rev. Lett.* **2004**, *93*, 146104.
(33) Pedersen, T. M.; Li, W. X.; Hammer, B. *Phys. Chem. Chem. Phys.* **2006**, *8*, 1566.

dx.doi.org/10.1021/ja2114163 | *J. Am. Chem. Soc.* 2012, 134, 5036−5039